1-1-2007

Mimicking phosphorylation of alphaB-crystallin affects its chaperone activity

Heath W. Ecroyd
University of Wollongong, heathe@uow.edu.au

Sarah Meehan

J Horwitz

Andrew Aquilina
University of Wollongong, aquilina@uow.edu.au

J L Benesch

See next page for additional authors

Mimicking phosphorylation of alphaB-crystallin affects its chaperone activity

Authors

Heath W. Ecroyd, Sarah Meehan, J Horwitz, Andrew Aquilina, J L Benesch, C V Robinson, Cait MacPhee, and John Carver

Biochemical Journal Immediate Publication. Published on 23 Aug 2006 as manuscript BJ20060981

Mimicking phosphorylation of alphaB-crystallin affects its chaperone activity

Heath Ecroyd*, Sarah Meehan*, Joseph Horwitz†, J. Andrew Aquilina‡, Justin L. P. Benesch§, Carol V. Robinson§, Cait E. MacPhee‖ and John A. Carver*,[1].

*School of Chemistry and Physics, The University of Adelaide, Adelaide, S. A. 5005, Australia, †Jules Stein Institute, U. C. L. A School of Medicine, Los Angeles, California 90095-7008, U. S. A., ‡School of Biological Sciences, University of Wollongong, Wollongong, N. S. W. 2522, Australia, §Department of Chemistry, University of Cambridge, Cambridge, CB2 1EW, U. K. and the ‖Biological and Soft Systems Group, Cavendish Laboratory, University of Cambridge, CB3 0HE, U. K.

Running Title; Chaperone activity of phosphomimics of αB-crystallin

[1] **Correspondence and reprint requests**:
School of Chemistry and Physics, The University of Adelaide, Adelaide, SA 5005, Australia, Tel. +61 8 830 33110; Fax. +61 8 830 34380; E-mail: john.carver@adelaide.edu.au

Biochemical Journal Immediate Publication. Published on 23 Aug 2006 as manuscript BJ20060981

Abstract

AlphaB-crystallin is a member of the small heat shock protein (sHsp) family that prevents misfolded target proteins from aggregating and precipitating. Phosphorylation at three serine residues (S19, S45 and S59) is a major post-translational modification that occurs to αB-crystallin. In this study, we produced recombinant proteins designed to mimic phosphorylation of αB-crystallin by incorporating a negative charge at these sites. We employed these mimics to undertake a mechanistic and structural investigation of the effect of phosphorylation on the chaperone activity of αB-crystallin to protect against two types of protein misfolding, i.e. amorphous aggregation and amyloid fibril assembly. We show that mimicking phosphorylation of αB-crystallin results in more efficient chaperone activity against both heat-induced and reduction-induced amorphous aggregation of target proteins. Mimicking phosphorylation increased the chaperone activity of αB-crystallin against one amyloid forming target protein (κ-casein), but decreased it against another (ccβ-Trp peptide). We observed that both target protein identity and solution (buffer) conditions are critical factors in determining the relative chaperone ability of wild-type and phosphorylated αB-crystallin. This study provides evidence for the regulation of the chaperone activity of αB-crystallin by phosphorylation and indicates that this may play an important role in alleviating the pathogenic effects associated with protein conformational diseases.

Keywords: small heat shock protein, amyloid, alphaB-crystallin, protein aggregation, chaperone, phosphorylation

Abbreviations used: αB-WT, wild-type αB-crystallin; αB-1P, S19D αB-crystallin; αB-2P, S14D/S45D αB-crystallin; αB-3P, S19D/S45D/S59D αB-crystallin; ADH, alcohol dehydrogenase; ANS, 8-anilino-1-napthalene sulphonate; Cat, catalase; DTT, 1,4-dithiothreitol; FRET, fluorescence resonance energy transfer; FPLC, fast protein liquid chromatography; MALS, multi angle light scattering; NMR, nuclear magnetic resonance; NOESY, nuclear overhauser effect spectroscopy; RCM, reduced and carboxymethylated; SEC, size exclusion chromatography; sHsp, small heat shock proteins; SDS-PAGE, sodium dodecyl sulfate-polyacrylamide gel electrophoresis; ThT, thioflavin T; TOCSY, total correlated spectroscopy; TEM, transmission electron microscopy.

Biochemical Journal Immediate Publication. Published on 23 Aug 2006 as manuscript BJ20060981

Introduction

During a protein's life cycle, exposure to conditions of physiological stress (e.g. heat, changes in pH, oxidation) can lead to destabilisation and formation of partially folded intermediates that expose hydrophobic regions to solution, which may interact resulting in large-scale aggregation and precipitation. Small heat shock proteins (sHsps) act in a chaperone manner to confer protection against cellular stress by recognising, interacting with and stabilising partially unfolded intermediates that have entered this "protein off-folding pathway" [1]. However, unlike the classical bacterial chaperonin GroEL, sHsps including αB-crystallin do not directly participate in refolding of the partially unfolded proteins, except in the presence of another chaperone protein, e.g. Hsp70 [2, 3]. In many cases, protein aggregation and precipitation are highly deleterious to cell viability and are the hallmark of diseases generally classified as protein misfolding or conformational diseases, e.g. Parkinson's, Alzheimer's and Creutzfeldt-Jakob diseases and cataract. As such, sHsps are thought to play a key role in preventing or alleviating diseases characterized by protein misfolding and aggregation [4-6].

αB-Crystallin is a sHsp primarily found in the eye lens, where it associates with the closely related αA-crystallin to form large hetero-oligomeric species. However, αB-crystallin is also constitutively expressed in many non-lenticular tissues, including the brain, lung and cardiac and skeletal muscle [7]. As with other members of the sHsp family, the expression of αB-crystallin is dramatically up-regulated in response to stress and pathological conditions [4, 8-10]. Both inside and outside the lens, a major posttranslational modification described for αB-crystallin is phosphorylation at three serine residues (S19, S45 and S59) [11, 12], which is mediated by at least two distinct mitogen-activated protein kinase enzymes [11-14].

Various types of cellular stress, such as heat, oxidation and increased intracellular calcium levels, stimulate the phosphorylation of αB-crystallin [11, 15]. In the lens, phosphorylation also increases with age, however, even in the young lens, αB-crystallin may be extensively phosphorylated [16-18]. In the brain, some of the αB-crystallin isolated from the proteinaceous aggregates of patients with degenerative diseases [19], amyloid plaques and Lewy bodies is phosphorylated [20]. However, it

Biochemical Journal Immediate Publication. Published on 23 Aug 2006 as manuscript BJ20060981

is not known whether there is a preference for the phosphorylated forms of αB-crystallin to interact with the proteins associated with these deposits.

A limited number of studies have investigated the role of phosphorylation on the chaperone action of αB-crystallin and only against amorphously aggregating proteins. Studies performed *in vitro* have used either purified forms of the phosphorylated protein from lenses, or recombinant proteins that have been designed to mimic serine phosphorylation by replacing it with a negatively charged aspartic or glutamic acid at the same position. One study, using bovine lenses and isoelectric focusing to obtain non-phosphorylated and phosphorylated αB-crystallin, showed a 60% reduction in the ability of the phosphorylated forms to prevent the cytochalasin-D induced depolymerisation of actin from filaments compared to the non-phosphorylated form [21]. Another employing ion-exchange chromatography to purify monophosphorylated αB-crystallin from bovine lenses, reported a 30% decrease in the ability of this form to prevent the heat-induced aggregation of β_L-crystallin [22]. Studies using phosphorylation mimics have indicated that an increase in phosphorylation leads to a decrease in the oligomerization of the protein [23] and a disruption in dimeric substructure within the oligomer [24]. One of these studies showed a slight decrease in the ability of a triple phosphorylation mutant (S19D/S45D/S59D) to prevent the thermal aggregation of lactate dehydrogenase or to refold denatured firefly luciferase, compared to the wild-type recombinant protein [23]. The other reported that, when used in a reduction assay of α-lactalbumin, the double phosphorylation mimic (S19D/S45D) promoted rather than inhibited protein precipitation [24], which was ascribed to co-aggregation and precipitation of reduced α-lactalbumin and the chaperone to form a higher molecular weight species [24]. This may be due to the phosphorylation mimics having an increased binding affinity to destabilised target proteins compared to the wild-type protein [25], however, it would be expected that this would lead to an increase in chaperone function rather than a decrease. Thus, the overall effect of phosphorylation on the function of αB-crystallin remains controversial and it for this reason that we sought to readdress this issue.

In this study, we have used recombinant proteins designed to mimic phosphorylation of αB-crystallin (S19D; αB-1P, S19D/S45D; αB-2P and S19D/S45D/S59D; αB-3P)

to undertake a comprehensive survey of their relative chaperone activity against different types of protein aggregation, i.e. disordered amorphous aggregation and ordered amyloid fibril formation. Amyloid fibril aggregation leads to highly structured cross β-sheet fibrillar arrays of proteins that can be observed as thread-like structures, sometimes assembled further into larger aggregates or plaques [26, 27]. They are characteristic of the protein deposits formed in diseases such as Alzheimer's, Parkinson's and Creutzfeldt-Jakob disease. In general, we found that phosphorylation of αB-crystallin leads to an increase in the chaperone activity of the protein against aggregating target proteins. However, the target protein and solution conditions were found to be important factors that regulate the effect of phosphorylation on the chaperone action of αB-crystallin. Using a variety of biophysical techniques, structural characterisation and comparison of the phosphorylation mimics and the wild-type protein were also undertaken.

Materials and Methods

Proteins including κ-casein and α-lactalbumin from bovine milk, bovine pancreas insulin, bovine liver catalase and yeast alcohol dehydrogenase were obtained from Sigma Chemical Co. (St. Louis, MO, U. S. A.) and used without further purification. Prior to use, the κ-casein was reduced and carboxymethylated as described earlier [28]. The 18mer coiled-coil α-helical peptide described previously [29], with additional C-terminal tryptophan residue (ccβ-Trp) was synthesized by CS Bio Co. (San Carlos, CA, U. S. A.). Bovine β_L-crystallin was purified via size exclusion chromatography (SEC) using methods described elsewhere [17, 30]. Thioflavin T (ThT), 8-anilino-1-napthalene sulphonate (ANS), 1,4-dithiothreitol (DTT) and β-mercaptoethanol were obtained from Sigma. Uranyl acetate was obtained from Agar Scientific (Essex, U. K.). Wild-type αB-crystallin (αB-WT) and its phosphorylation mimics (αB-1P, αB-2P, αB-3P) were expressed and purified as described previously [24, 30]. SDS-PAGE analysis of the purified αB-crystallin proteins indicated that they contained less than 5% contaminating proteins. The concentrations of proteins used in these studies were determined by protein assays based on the Bradford method (Bio-Rad, Herts, U. K.) and/or by spectrophotometric methods using a Cary 5000 UV/Vis spectrophotometer (Varian, Melbourne, Australia) and calculated extinction coefficients based on amino acid sequences.

Biochemical Journal Immediate Publication. Published on 23 Aug 2006 as manuscript BJ20060981

Intrinsic and extrinsic fluorescence

Intrinsic tryptophan fluorescence spectra were recorded using a Cary Eclipse fluorescence spectrophotometer (Varian) equipped with temperature control. The excitation wavelength was set at 295 nm and emission was monitored between 300-400 nm. The excitation and emission slit widths were set at 5 nm. The αB-WT and phosphorylation mimics were measured at 100 μg/mL in 50 mM phosphate buffer, pH 7.2 or 100 mM ammonium acetate buffer, pH 6.8. Samples were maintained at the designated temperatures for 30 mins before being assayed.

For the 8-anilinonapthelene-1-sulfonate (ANS) binding studies, a stock solution of methanolic ANS (100 mM) was diluted 1000-fold into a 100 μg/mL protein solution in 50 mM phosphate buffer, pH 7.2. Emission fluorescence spectra were monitored (400-600 nm) following excitation at 350 nm. Fluorescence resonance energy transfer (FRET) analysis was performed on the same samples by excitation at 295 nm and monitoring the emission fluorescence spectra (320-560 nm). The excitation and emission slit widths for these studies were set at 5 nm. Samples were maintained at the designated temperatures for 30 mins before being assayed.

Chaperone activity assays

The aggregation and precipitation of the target proteins, incubated in the presence of increasing amounts of the αB-crystallins and monitored by either ThT fluorescence or turbidity assay (see below), were performed in duplicate using a 96-microwell plate. At the end of the assay the samples were collected and centrifuged (15,000 g, 15 mins) to separate the soluble and insoluble (pellet) fractions. The pellet was washed with an equal volume of the same buffer used in the aggregation assay.

Thioflavin T assays

The formation of amyloid fibrils by target proteins was monitored using an *in situ* ThT binding assay method adapted from [31]. We used two model target proteins that form amyloid fibrils under physiological conditions, reduced and carboxymethylated κ-casein (RCMκ-casein) and ccβ-Trp. RCMκ-Casein (500 μg/mL) and ccβ-Trp (150 μg/mL) were incubated at 37 °C in 50 mM phosphate buffer, pH 7.2 and 50 mM

Biochemical Journal Immediate Publication. Published on 23 Aug 2006 as manuscript BJ20060981

phosphate buffer, pH 7.8 respectively. In order to assess the effect of pH, in some experiments RCMκ-casein was incubated at 37 °C in 50 mM phosphate buffer, pH 7.8 (the same pH as that used with ccβ-Trp). Samples were prepared in duplicate and incubated with 10 μM ThT in a 96-microwell plate. The plates were sealed to prevent evaporation and the fluorescence levels measured with a Fluostar Optima plate reader (BMG Labtechnologies, Melbourne, Australia) with a 440/490 nm excitation/emission filter set. The change in ThT fluorescence measured after its initial decrease (due to an increase in temperature from room temperature to 37 °C) is presented. The change in ThT fluorescence in the absence of the target protein was negligible for each assay.

Turbidity assays

Light scattering at 340 nm was measured and recorded using a Fluostar Optima plate reader (BMG Labtechnologies). The change in light scattering at 340 nm for each sample is presented in the graphs. The change in light scattering in the absence of the target protein was negligible for each assay.

Heat-stress assay

Bovine liver catalase (500 μg/mL) or bovine β_L-crystallin (500 μg/mL) was incubated at 60 °C in 50 mM phosphate buffer, pH 7.2. Alcohol dehydrogenase from yeast (500 μg/mL) was incubated at 42 °C in 50 mM phosphate buffer, pH 7.2 with 100 mM NaCl and 2 mM EDTA.

Reduction assay

Bovine pancreas insulin (250 μg/mL) was incubated at 37 °C in 50 mM phosphate buffer, pH 7.2 and α-lactalbumin (500 μg/mL) was incubated at 37 °C in 50 mM phosphate buffer, pH 7.2 containing 100 mM NaCl or in 100 mM ammonium acetate, pH 6.8. Aggregation and precipitation was initiated by addition of DTT to a final concentration of 10 mM (insulin) or 20 mM (α-lactalbumin).

Biochemical Journal Immediate Publication. Published on 23 Aug 2006 as manuscript BJ20060981

SDS-PAGE

SDS-PAGE was conducted on 15% or 20% acrylamide gels (v/v) using standard techniques. Samples were mixed with an equal volume of reducing gel sample buffer such that the final concentration of 2-mercaptethanol was 2.5% (v/v), and then heated (95 °C, 5 min) before loading on to gels.

Size-exclusion FPLC and light scattering

Size exclusion chromatography of samples (100 μL) was performed on a Superdex 200HR 10/30 column (Amersham Biosciences, Buckinghamshire, U.K.) and eluted at 0.4 mL/min with the corresponding buffer used in the aggregation assay, i.e. 50 mM phosphate buffer, pH 7.2. The column was calibrated with gel filtration markers (Bio-Rad).

Size exclusion chromatography coupled with multi-angle light scattering (SEC-MALS) was performed using a Superose 6HR 10/30 column (Amersham Biosciences) and a DAWN EOS multiangle laser light scattering detector (Wyatt Technology, Santa Barbara, CA, U. S. A.). Samples were loaded on to the column at a concentration of 1.5 mg/mL and eluted with 100 mM ammonium acetate, pH 6.8 or 50 mM phosphate buffer, pH 7.2 containing 100 mM NaCl at a flow rate of 0.5 mL/min.

Transmission electron microscopy (TEM)

Formvar and carbon-coated nickel electron microscopy grids were prepared by the addition of 2 μL of protein sample, washed with 3 x 10 μL of milli-Q and negatively stained with 10 μL of uranyl acetate (2% w/v). Samples were viewed using a Philips CM100 transmission electron microscope (Philips, Eindhoven, Netherlands) at a magnification range of 25,000-64,000 using an 80 kV excitation voltage.

Temperature-dependent denaturation

The thermal stability of the αB-crystallin proteins (250 μg/mL) in 50 mM phosphate buffer, pH 7.2 containing 100 mM NaCl or in 100 mM ammonium acetate buffer, pH 6.8 was monitored by measuring the light scattering of the sample at 360 nm using a

Biochemical Journal Immediate Publication. Published on 23 Aug 2006 as manuscript BJ20060981

Cary 5000 UV/Vis spectrophotometer equipped with a Peltier temperature controller. The temperature of the samples was increased at a rate of 1 °C/min. The change in absorbance at 360 nm is presented in the graphs.

Mass spectrometric analysis

Nanoelectrospray mass spectrometry experiments were performed on a Q-Tof II spectrometer (Micromass UK Ltd.) that has been modified for high mass operation [32]. Conditions were the same as those described previously [24, 33].

NMR spectroscopy

^{1}H-NMR spectra were acquired at 600 MHz on a Varian Inova-600 NMR spectrometer with the parameters outlined in [34] except that the sweep width was 6000 Hz. The mixing time in the NOESY spectrum was 100 ms and the spin lock period in the TOCSY spectrum was 60 ms. The concentration of αB-WT and αB-3P was 10 mg/mL dissolved in 10 mM phosphate buffer, pH 7.0 and 10% D_2O/90% H_2O (v/v).

Results

Structural analyses of wild-type αB-crystallin and its phosphorylation mimics.

We examined, using a variety of biophysical techniques, the structure of the recombinant phosphorylation mimics compared to that of the recombinant wild-type protein. Intrinsic tryptophan fluorescence of the proteins measured at 37 °C showed that both αB-WT and αB-3P had similar emission intensities, although the λ_{max} of αB-3P was slightly longer (αB-WT-340 nm, αB-3P– 342 nm) and the fluorescence emission intensity slightly lower than αB-WT (Fig. 1A) indicating that the tryptophan residues in αB-3P are slightly more solvent exposed under these conditions. The αB-2P mimic (λ_{max} 343 nm) had the highest and αB-1P (λ_{max} 339 nm) the lowest fluorescence emission intensities at 37 °C. After heating to 60 °C, the fluorescence emission intensity decreased and the λ_{max} shifted to longer wavelengths for all the proteins (Fig. 1B). The biggest relative decrease in emission intensity and largest shift in λ_{max} was for αB-3P (λ_{max} 346 nm) indicating that the environment of its tryptophan residues changed the most upon heating (i.e. they become more solvent exposed).

Biochemical Journal Immediate Publication. Published on 23 Aug 2006 as manuscript BJ20060981

The ANS fluorescence emission spectra measured at 37 °C showed little difference in exposed, clustered hydrophobicity between αB-WT, αB-1P and αB-3P (Fig. 1C). In contrast, αB-2P had a lower fluorescence emission intensity indicating that it exposes fewer clustered regions of hydrophobicity, i.e. it is more folded under these conditions. At 60 °C, the fluorescence emission intensity decreased and λ_{max} moved to longer wavelengths for all the proteins, reflecting a loss of exposed hydrophobicity as the proteins unfold (Fig. 1D). Again, αB-3P showed the biggest decrease in fluorescence intensity upon heating suggesting that it unfolds the most readily.

We next conducted FRET analysis in order to probe dynamic structural changes in the proteins. FRET is a technique to study conformational changes in proteins in which the emission of tryptophan residues (at around 350 nm) is used to excite nearby ANS fluorophores. FRET was shown for all proteins by a decrease in the tryptophan fluorescence and a concomitant increase in their normal ANS fluorescence (compare Fig. 1A-D with Fig. 1E and F). At 37 °C, αB-WT, αB-1P and αB-3P all had comparable levels of FRET indicating that the tryptophan residues are in close proximity to the clustered regions of exposed hydrophobicity in each of these proteins. The αB-2P had lower levels of FRET indicating an increase in the distance between its tryptophan residues and hydrophobic regions compared to the other proteins. The FRET for each protein decreased after heating to 60 °C, which is indicative of an increase in the distance between these tryptophan residues and the surrounding hydrophobic sites due to unfolding of the protein.

Nanoelectrospray mass spectrometry was used to compare the oligomeric distributions of αB-WT and αB-3P. As has been previously shown for this polydisperse protein, the mass spectra exhibited broad peaks and an elevated baseline, consistent with the overlap of peaks arising from a multitude of different sized constituent oligomers [24]. In this case, the αB-WT spectrum contained a mixture of broad and sharp peaks between 7,000 and 13,000 *m/z*. In contrast, peaks in the spectrum of αB-3P were less well defined over the same *m/z* range and were superimposed upon a significantly elevated baseline (Fig. 2A). The fact that this baseline elevation continues beyond 14,000 *m/z* suggests that the range of oligomers in αB-3P extends to a much higher mass range than the WT protein. The major peaks

Biochemical Journal Immediate Publication. Published on 23 Aug 2006 as manuscript BJ20060981

in the spectra for αB-WT and αB-3P were 10,080 *m/z* and 10,200 *m/z* respectively, corresponding to the species at which all oligomers carry two charges per subunit. These peaks were isolated using a tandem mass spectrometry approach that enables the relative quantification of the constituent oligomers within assemblies [24], and it was found that the highest relative proportion of subunits in an oligomer for both αB-WT and αB-3P was 28 (Fig. 2B). Both proteins form major oligomers of between 24 to 32 subunits, however there is a clear bias toward oligomers with an even number of subunits in αB-WT that is not apparent in αB-3P. Furthermore, in the case of αB-3P, the distribution of minor oligomers around the median was skewed toward those containing larger numbers of subunits (not shown).

^{1}H-NMR spectroscopy was undertaken on αB-WT and αB-3P to investigate structural differences between the proteins. Cross-peaks from the highly mobile flexible C-terminal extension of 12 amino acids [35] were observed in ^{1}H-NMR TOCSY and NOESY spectra of both αB-WT and αB-3P (data not shown). No extra cross-peaks were observed in the αB-3P spectra compared to those of αB-WT, indicating that no additional regions of marked flexibility are present in αB-3P compared to αB-WT. However, the intensity of the cross-peaks in the spectra of αB-3P was reduced implying a slightly reduced flexibility of its C-terminal extension compared to αB-WT. This may reflect structural alterations in the domain core of αB-3P compared to αB-WT, which lead to αB-3P having a much larger mass range than αB-WT (see below).

The effect of mimicking phosphorylation on the chaperone activity of αB-crystallin against aggregating target proteins.

Amyloid fibril assembly

We employed two different models to examine the effect of phosphorylation on the ability of αB-crystallin to prevent ordered protein aggregation in the form of amyloid fibril formation: reduced and carboxymethylated κ-casein (RCMκ-casein), an unstructured protein in its native state; and ccβ-Trp, a modified form of the ccβ peptide that exists in a triple-helical coiled-coil configuration in its native state (data not shown). Importantly, both form amyloid fibrils under physiological conditions [29, 36] and so are of relevance to amyloid formation by aggregating proteins *in vivo*.

Biochemical Journal Immediate Publication. Published on 23 Aug 2006 as manuscript BJ20060981

Fibril formation by RCMκ-casein (500 μg/mL), as monitored by an increase in ThT binding, showed a gradual increase over the time course of the assay (Fig. 3A). Analysis of RCMκ-casein by SEC before fibril formation showed that it predominately exists as a high molecular mass oligomer of more than 1 MDa and a species of apparent mass of ~40 kDa, corresponding to the κ-casein dimer (Fig. 3B). After fibril assembly only a single peak that eluted in the void volume of the column was evident indicating that most of the protein exists in high molecular weight species. The addition of αB-WT (500 μg/mL) (1.0: 1.0 molar ratio of RCMκ-casein: αB-crystallin) to the sample resulted in a decrease in ThT binding (Fig. 3A). Size-exclusion chromatography indicated the formation of a high molecular mass complex between these two proteins since αB-WT alone had a calculated average molecular mass of ~600 kDa and this peak shifted to an earlier elution time in the presence of RCMκ-casein. The RCMκ-casein high molecular mass peak that eluted in the void volume of the column was reduced significantly in the presence of αB-WT (Fig. 3B). The phosphorylation mimics were more effective in preventing the increase in ThT binding associated with fibril formation by RCMκ-casein and αB-3P completely abolished it (Fig. 3A). The SEC data showed that αB-3P elutes later (~430 kDa average molecular mass) and as a broader peak than αB-WT. A high molecular mass complex between αB-3P and RCMκ-casein was evidenced by the shift in the elution peaks of the individual components to earlier elution times (Fig. 3B). Altering the pH of the buffer in the *in situ* ThT assay to that used for ccβ-Trp (i.e. pH 7.8, see below) had no effect on the overall trends in these data (data not shown).

Electron micrographs of negatively stained RCMκ-casein fibrils showed them to be thread-like structures, approximately 100-900 nm in length (Fig. 4A), similar to those reported previously [36]. In the presence of the αB-crystallins the number and length of these fibrils appeared to be reduced. In the presence of αB-WT, short prefibrillar species approximately 50-100 nm in length were observed (Fig. 4B), although the predominant species were large amorphous aggregates similar to those seen when the αB-crystallins were incubated alone (data not shown). No fibrillar or prefibrillar species were observed by TEM in samples incubated in the presence of αB-3P (Fig. 4C), or the other phosphorylation mimics (data not shown). These samples only

Biochemical Journal Immediate Publication. Published on 23 Aug 2006 as manuscript BJ20060981

contained amorphous aggregates, similar to those seen for RCMκ-casein before incubation [36], or when the αB-crystallins were incubated alone (data not shown).

We next tested the chaperone activity of the phosphorylation mimics against an extended form of ccβ. At 37 °C, the increase in ThT fluorescence associated with fibril formation by ccβ-Trp (150 μg/mL) was sigmoidal and included a lag phase of 150 mins followed by a growth phase, which reached a plateau after approximately 600 mins (Fig. 5A). The presence of the αB-crystallins at 130 μg/mL (a 1.0: 0.1 molar ratio of ccβ-Trp: αB-crystallin) decreased ThT fluorescence and therefore by inference peptide self-assembly, such that it was almost completely abolished in the presence of αB-WT (Fig. 5A). Similarly, SDS-PAGE of pelleted material demonstrated that ccβ-Trp precipitates from solution when incubated in the absence of the chaperone protein (Fig. 5B), whereas in the presence of αB-WT the peptide remains soluble. Increasing the number of negative charges used to mimic phosphorylation of αB-crystallin decreased the protective action of the chaperone in terms of ThT binding (Fig. 5A) and increased the proportion of ccβ-Trp that precipitated from solution (Fig. 5B).

Electron micrographs of ccβ-Trp after incubation demonstrated the formation of unbranched amyloid fibrils varying in length between 100-700 nm (Fig. 6A). In the presence of αB-WT, only a small number of fibrils were observed by TEM (Fig. 6B), and those that were present appeared to have a different morphology to those typical of ccβ-Trp alone, i.e. thinner, more cylindrical fibrils were observed as well as thread-like tangles (Fig. 6B and C). When ccβ-Trp was incubated with αB-3P, both types of fibrils were apparent, i.e. both long, straight fibrils typical of those adopted by the ccβ-Trp peptide alone (Fig. 6D), and thin, thread-like tangles of fibrils seen in the presence of αB-WT (Fig. 6E).

Heat-induced amorphous aggregation

The effect of phosphorylation on the ability of αB-crystallin to prevent amorphous aggregation was examined by employing the heat-induced aggregation of the target proteins, β_L-crystallin (a natural target of αB-crystallin in the lens), catalase and

Biochemical Journal Immediate Publication. Published on 23 Aug 2006 as manuscript BJ20060981

alcohol dehydrogenase (Fig. 7). Turbidity was monitored by measuring the change in absorbance due to light scattering at 340 nm. When β_L-crystallin (500 μg/mL) was incubated in the absence of the αB-crystallins, a marked increase in light scattering due to protein precipitation occurred after an initial lag phase of 20 mins and plateaued after 70 mins (Fig. 7A). After 80 mins, the majority of the β_L-crystallin had precipitated from solution (Fig. 7B). All the αB-crystallins (100 μg/mL) were effective at suppressing heat-induced aggregation of β_L-crystallin (a 1.0: 0.2 molar ratio of β_L-crystallin: αB-crystallin), however the phosphorylation mimics were more effective than αB-WT and αB-3P was the most effective. Similarly, whereas in the presence of αB-WT a small amount of β_L-crystallin was present as an insoluble species (Fig. 7B), the addition of the phosphorylation mimics resulted in β_L-crystallin only being detected in the soluble fraction of the sample.

When catalase (500 μg/mL) was incubated at 60 °C in the absence of the αB-crystallin proteins after an initial lag phase of 18 mins a large increase in light scattering was observed which plateaued by 45 mins (Fig. 7C). After 80 mins, most of the catalase precipitated from solution as indicated by SDS-PAGE (Fig. 7D). The presence of the αB-crystallins (100 μg/mL) (a 1.0: 0.6 molar ratio of catalase: αB-crystallin) increased the lag phase (to 21 mins) and reduced the magnitude of light scattering due to protein precipitation. In the presence of αB-WT there was a decrease in the proportion of catalase that pelleted from solution (Fig. 7D). Increasing the number of negative charges designed to mimic phosphorylation of αB-crystallin increased the chaperone's protective ability such that all of the catalase remained soluble after 80 mins in the presence of αB-1P, αB-2P and αB-3P. Interestingly, in this example and other cases described below, when insoluble precipitate was formed in the presence of the chaperone proteins (e.g. catalase incubated in the presence of αB-WT), it was made up of both the target protein and chaperone. This suggests that, in attempting to prevent aggregation, αB-crystallin may become saturated and co-aggregate with the target proteins leading to their co-precipitation.

Alcohol dehydrogenase (500 μg/mL), incubated at 42°C in the absence of the αB-crystallins, after a lag phase of 15 mins showed a large increase in light scattering that

Biochemical Journal Immediate Publication. Published on 23 Aug 2006 as manuscript BJ20060981

plateaued after 80 mins (Fig. 7E). After 100 mins, most of the alcohol dehydrogenase was still soluble in solution, however, some was insoluble as evidenced by SDS-PAGE (Fig. 7F). All of the αB-crystallins (50 μg/mL) (a 1.0: 0.2 molar ratio of alcohol dehydrogenase: αB-crystallin) inhibited the increase in light scattering due to the heat-induced aggregation of alcohol dehydrogenase; the phosphorylation mimics were more effective than αB-WT (Fig. 7E). The presence of the αB-crystallins resulted in none of the alcohol dehydrogenase being detected in the insoluble fraction when it was analysed by SDS-PAGE (Fig. 7F).

Reduction-induced amorphous aggregation

DTT induced aggregation of insulin (250 μg/mL) commenced after 10 mins and reached a plateau after 45 mins (Fig. 8A). After 80 mins, the majority of the B-chain of insulin in the sample existed as a precipitate, whilst the A-chain, which is resistant to DTT-induced aggregation [37], remained soluble (Fig. 8B). In the presence of αB-WT (125 μg/mL) (a 1.0: 0.15 molar ratio of insulin: αB-crystallin), the degree of light scattering was only slightly reduced. At the same ratios, the phosphorylation mimics were much more effective at preventing the precipitation of the insulin B-chain; αB-2P and αB-3P inhibited the increase in light scattering the most (Fig. 8A).

In the case of the DTT-induced aggregation of α-lactalbumin, the effect of phosphorylation on αB-crystallin's chaperone activity was found to be dependent on the solution conditions. When α-lactalbumin (500 μg/mL) was reduced and precipitated in 50 mM phosphate buffer, pH 7.2 containing 100 mM NaCl, αB-2P and αB-3P (250 μg/mL) (a 1.0: 0.3 molar ratio of α-lactalbumin: αB-crystallin) were most effective in suppressing the light scattering associated with protein precipitation (Fig. 8C). SDS-PAGE indicated that a higher proportion of the target and chaperone protein remained soluble as the number of negative charges that mimic phosphorylation of αB-crystallin increased (Fig. 8D). The opposite trend was observed when α-lactalbumin (500 μg/mL) was reduced by DTT in 100 mM ammonium acetate buffer (pH 6.8) (Fig. 8E). The increase in light scattering associated with precipitation of α-lactalbumin commenced 15 mins after the addition of DTT and reached a plateau after 50 mins. Not all of the α-lactalbumin precipitated

Biochemical Journal Immediate Publication. Published on 23 Aug 2006 as manuscript BJ20060981

under these conditions as evidenced by SDS-PAGE (Fig. 8F). In the presence of αB-WT (250 μg/mL), the aggregation was initially suppressed, but the degree of light scattering increased after 25 mins such that after 80 mins it was greater then when α-lactalbumin was incubated in the absence of the chaperone. When analysed by SDS-PAGE, both α-lactalbumin and αB-WT were found in the pellet indicating that they interact and then co-precipitate (Fig. 8F). The increase in light scattering was more rapid in the presence of the phosphorylation mimics (Fig. 8E) and, as the number of negative charges that mimic phosphorylation increased, less of the chaperone protein remained in solution, such that none of αB-3P was soluble after 80 mins (Fig. 8F). Whilst pH changes were found to have a significant effect on the rate of aggregation of α-lactalbumin (for example, changing the pH of the ammonium acetate buffer from pH 6.8 to 7.2 increased the lag phase in the aggregation curve by 20 mins and decreased the light scattering due to protein precipitation by 40%), the overall trends in chaperone ability of the αB-crystallins to prevent its aggregation in each buffer were the same.

Mimicking phosphorylation of αB-crystallin affects its thermal stability and oligomeric distribution.

In order to decipher the differences observed in the relative ability of the wild-type and phosphorylation mimics to chaperone reduced α-lactalbumin under different solution conditions (Figs. 8C and 8E), we examined the stability of the chaperone proteins in the different buffers used in these assays. In phosphate buffer (50 mM, pH 7.2 containing 100 mM NaCl), αB-WT underwent two temperature-dependent structural transitions, one at 65 °C and another at 78 °C (Fig. 9A). In contrast, αB-3P did not undergo a significant thermal transition until 82 °C (Fig, 9A). However, when incubated in ammonium acetate buffer (100 mM, pH 6.8), αB-3P was significantly less stable than αB-WT; most of αB-3P precipitated from solution at 63 °C compared to around 78 °C for αB-WT (Fig. 9B). The intrinsic tryptophan fluorescence of αB-WT or αB-3P was not different when incubated in either the phosphate or ammonium acetate buffers (data not shown) indicating that the difference in stability is not due to a detectable unfolding of αB-3P in the ammonium acetate buffer.

Biochemical Journal Immediate Publication. Published on 23 Aug 2006 as manuscript BJ20060981

We therefore investigated differences in the oligomeric distribution of αB-WT and αB-3P in these two buffer systems. When incubated in 50 mM phosphate buffer pH 7.2, both proteins elute as a symmetrical peak, although αB-3P eluted much later than αB-WT (Fig. 3). Horwitz [38] has previously shown by SEC-MALS that under these conditions αB-WT exists within the range of 480-640 kDa, with an average molecular mass of 580 kDa. Upon introduction of three negative charges that mimic phosphorylation this range increases (320-730 kDa) and average molecular mass decreases (440 kDa). In contrast, when these proteins are incubated in ammonium acetate, αB-WT exists within the range of 400-780 kDa, with an average molecular mass of 530 kDa (Fig. 9C) and, whilst αB-3P has the same average molecular mass as αB-WT (530 kDa), it is much more polydisperse (330-950 kDa), in a similar manner to that reported for αB-1P and αB-2P [24].

Discussion

The negative charge introduced into the recombinant αB-crystallin by replacing the serine residues with aspartate is designed to mimic the natural phosphorylation state of the protein. This method has been employed previously for αB-crystallin and shown to have similar effects as endogenously phosphorylated αB-crystallin in regards its oligomeric distribution [23], subcellular localization [39] and cellular trafficking [40]. Thus, using this rationale we have employed αB-crystallin phosphomimics to investigate the chaperone action of αB-crystallin on amyloid fibril formation and amorphous aggregation. Our results show that the negative charges introduced into αB-crystallin by phosphorylation has a major effect on its chaperone ability against target proteins undergoing both types of aggregation.

In αB-crystallin, the three sites of phosphorylation are in the N-terminal domain of the protein, outside of the conserved C-terminal 'α-crystallin' domain. Intrinsic fluorescence shows that phosphorylation results in structural changes in the N-terminal domain of αB-crystallin. The αB-WT, αB-1P and αB-3P proteins all had very similar ANS and FRET fluorescence spectra at 37 °C indicative of similar regions of clustered hydrophobicity and their proximity to accessible tryptophan residues. Since αB-3P had the biggest change in ANS and FRET fluorescence upon

Biochemical Journal Immediate Publication. Published on 23 Aug 2006 as manuscript BJ20060981

heating from 37 °C to 60 °C, these data suggest that its structure is altered the most by heating, which may facilitate its higher affinity for heat-stressed target proteins used in this study. When incubated in phosphate buffer, αB-3P was found to be more thermostable than αB-WT (Fig. 9). Its relative instability in acetate buffer probably reflects the relatively higher destabilising effect of this ion on protein solubility compared to phosphate buffer, as indicated by the Hofmeister salt series [41]. With regards αB-crystallin, our results suggest that phosphorylation accentuates this difference in protein solubility in the presence of different buffer ions, which is supported by the data showing that αB-WT and αB-3P exist in different oligomeric distributions in different buffer systems and have a greater mass range in ammonium acetate (Fig. 9).

In an elegant study using destabilized T4 lysozyme mutants as models of partially folded, intermediate states of the protein, Koteiche and McHaourab [25] showed that serine to aspartate phosphorylation mimics of αB-crystallin have a higher binding affinity (and by inference chaperone ability) to these partially folded states of T4 lysozyme compared to the wild-type protein. It was concluded that, through phosphorylation, αB-crystallin binding is activated to levels that exceed the affinity and binding capacity of αA-crystallin for the T4L mutants [25] (αB-WT having a lower affinity for these mutants than αA-crystallin). Our results are consistent with this and other findings showing that phosphorylation increases the polydispersity of αB-crystallin, reduces its oligomeric size and diminishes its preference for assemblies with an even number of subunits [24, 38]. It has been proposed that αB-crystallin acts as a chaperone via a dimeric form that dissociates from the oligomer and interacts with the target proteins [1, 42]. This bicomponent, target protein-αB-crystallin complex is then incorporated back into the αB-crystallin oligomer. Aquilina et al. [24] suggested that, by analogy with the known structure of Hsp16.9, a related sHsp from wheat [42], the quaternary substructure of αB-crystallin is destabilised by phosphorylation of S45 because introduction of a negative charge at this site results in the disruption of intersubunit contacts by the α2 helix in the N-terminal domain. The increased prevalence of this dissociated state upon introduction of a negative charge at this site may be responsible for the enhanced chaperone activity of αB-2P and αB-3P seen against a number of target proteins used in this study, rather than a direct

Biochemical Journal Immediate Publication. Published on 23 Aug 2006 as manuscript BJ20060981

interaction of the phosphorylated site with the target protein [25]. This may occur in a similar manner to other treatments (i.e. elevated temperature, presence of denaturant), which lead to structural perturbation of the αB-crystallin oligomer, an increase in the exposure of hydrophobic surfaces and/or greater subunit exchange, and an enhancement of the overall chaperone activity of the protein.

Our results indicate that αB-crystallin inhibits pathways of protein aggregation that lead to the formation of amyloid fibrils. In the two systems studied, the presence of the chaperone inhibited the increase in ThT fluorescence associated with amyloid fibril formation [43]. From our results, αB-crystallin appears to inhibit the formation of fibrils in the early stages of aggregation since significantly fewer mature fibrils were observed in the presence of the chaperone, as judged by TEM. It possibly does so by interacting with intermediately folded states of the target protein to prevent the nucleation event that precedes fibril formation or by interacting with prefibrillar aggregates, which would be consistent with the findings that it forms a high molecular weight complex with the target protein (Fig. 3B) and that the complex remains in solution (Fig. 5B). αB-Crystallin effectively suppressed fibril formation by α-synuclein, the protein associated with Lewy bodies and plaque formation in Parkinson's disease, by interacting with α-synuclein early along its aggregation pathway [44]. Furthermore, it redirects α-synuclein from a fibril-forming pathway towards an amorphous aggregation pathway [44]. αB-Crystallin also interacts with apolipoprotein C-II at its early stage of aggregation to prevent large-scale fibril formation [45].

The effectiveness of αB-crystallin to act as a chaperone against a particular target protein is due, at least in part, to the different conformational states of the target protein's intermediately folded forms. This is because α-crystallin has a differential mode of binding to target proteins that reflects the latter's free-energy of unfolding [46]. The more destabilised and unfolded substrates have higher binding affinities to αB-crystallin [25]. This may account for the differences seen in the chaperone action of the phosphorylation mimics compared to wild-type αB-crystallin against the two fibril-forming proteins, RCMκ-casein and ccβ-Trp, used in this study. The ccβ-Trp peptide exists in a highly structured coiled-coil configuration in the native state

Biochemical Journal Immediate Publication. Published on 23 Aug 2006 as manuscript BJ20060981

compared to RCMκ-casein, which is essentially unstructured. Each protein's intermediate states may differ in their structure, hydrophobicity and binding affinity for αB-crystallin. Such factors may be responsible for the variation observed in the effect of phosphorylation of αB-crystallin on its ability to prevent fibril formation in these two different systems. Moreover, as a result of differences in intermediate states, variations in the chaperone ability of αB-crystallin against different target proteins are likely to arise.

Furthermore, the conditions under which aggregation occurs were also found to play an important role in the chaperone action of αB-crystallin. In the case of amorphously aggregating target proteins, in general we found that increasing the number of negative charges used to mimic phosphorylation of αB-crystallin increased its chaperone ability. However, our studies involving α-lactalbumin indicated that the effect of phosphorylation on αB-crystallin is also dependent upon the solution conditions under which aggregation occurred. This was shown to be due, at least in part, to the overall stability of the chaperone in solution (Fig. 9). By comparing the oligomeric distribution of the proteins in these buffer systems using SEC-MALS, it was observed that local structural perturbations between these proteins are further influenced by the surrounding medium. Co-aggregation and co-precipitation of αB-crystallin with the target protein probably results from the saturation of binding sites available for substrate interaction, those with higher affinities being saturated first. This phenomenon has also been observed with the R120G mutant of αB-crystallin, a destabilised form of the protein, which probably exposes more of its binding sites(s) to solution, enhancing the rate of reaction and leading to its co-precipitation when incubated with target proteins such as reduced α-lactalbumin [34, 47, 48]. Thus, although the protein is a more effective chaperone in terms of its binding affinities, under certain conditions this may lead to an apparent increase in light scattering, due to its saturation and co-precipitation. Such factors are important when assessing comparative affinities and function of sHsps and differences in assay conditions may explain the apparent disparate findings of previous studies looking at the effect of phosphorylation on the chaperone activity of αB-crystallin.

Biochemical Journal Immediate Publication. Published on 23 Aug 2006 as manuscript BJ20060981

It is not known how phosphorylation and dephosphorylation of αB-crystallin is regulated in the cell. Phosphorylation of αB-crystallin occurs under normal physiological conditions *in vivo* and is stimulated by stress [11, 15]. Thus, it would be predicted that the activity of αB-crystallin, a protein that is required to have high activity during stress conditions in the cell, would be enhanced by phosphorylation rather than lessened. It follows that phosphorylation may provide a molecular switch to the cell that serves to regulate the binding affinity of αB-crystallin, by disrupting its oligomeric state and increasing the amount of its 'activated' form. In summary, our results show that the introduction of negative charges brought about by phosphorylation of αB-crystallin has a significant effect on its structure and chaperone ability against target proteins undergoing either amorphous or amyloid fibril-type aggregation. Our results suggest that this highly prevalent post-translational modification of sHsps may play an important role in alleviating the pathogenic effects associated with protein conformational diseases.

Acknowledgements

This work was supported by grants (to JAC) from the National Health and Medical Research Council (NHMRC) of Australia and the Australian Research Council. HE is supported by an NHMRC Peter Doherty Postdoctoral Training Fellowship and SM was supported by a Royal Society International Fellowship. We thank Dr. Lyn Waterhouse (Medical School, University of Adelaide) for assistance with TEM and Drs. Glyn Devlin and Anna Tickler for help with the initial experiments involving ccβ-Trp.

References

1 Carver, J. A., Rekas, A., Thorn, D. C. and Wilson, M. R. (2003) Small heat-shock proteins and clusterin: intra- and extracellular molecular chaperones with a common mechanism of action and function? IUBMB Life **55**, 661-668

2 Ehrnsperger, M., Graber, S., Gaestel, M. and Buchner, J. (1997) Binding of non-native protein to Hsp25 during heat shock creates a reservoir of folding intermediates for reactivation. Embo J. **16**, 221-229

3 Jakob, U., Gaestel, M., Engel, K. and Buchner, J. (1993) Small heat shock proteins are molecular chaperones. J. Biol. Chem. **268**, 1517-1520

4 Clark, J. I. and Muchowski, P. J. (2000) Small heat-shock proteins and their potential role in human disease. Curr. Opin. Struct. Biol. **10**, 52-59

5 Macario, A. J. and Conway de Macario, E. (2005) Sick chaperones, cellular stress, and disease. N. Engl. J. Med. **353**, 1489-1501

6 Sun, Y. and MacRae, T. H. (2005) The small heat shock proteins and their role in human disease. FEBS J. **272**, 2613-2627

7 Kato, K., Shinohara, H., Kurobe, N., Inaguma, Y., Shimizu, K. and Ohshima, K. (1991) Tissue distribution and developmental profiles of immunoreactive alpha B crystallin in the rat determined with a sensitive immunoassay system. Biochim. Biophys. Acta. **1074**, 201-208

8 Klemenz, R., Frohli, E., Steiger, R. H., Schafer, R. and Aoyama, A. (1991) Alpha B-crystallin is a small heat shock protein. Proc. Natl. Acad. Sci. U. S. A. **88**, 3652-3656

9 Ochi, N., Kobayashi, K., Maehara, M., Nakayama, A., Negoro, T., Shinohara, H., Watanabe, K., Nagatsu, T. and Kato, K. (1991) Increment of alpha B-crystallin mRNA in the brain of patient with infantile type Alexander's disease. Biochem. Biophys. Res. Commun. **179**, 1030-1035

10 Kato, K., Inaguma, Y., Ito, H., Iida, K., Iwamoto, I., Kamei, K., Ochi, N., Ohta, H. and Kishikawa, M. (2001) Ser-59 is the major phosphorylation site in alphaB-crystallin accumulated in the brains of patients with Alexander's disease. J. Neurochem. **76**, 730-736

11 Ito, H., Okamoto, K., Nakayama, H., Isobe, T. and Kato, K. (1997) Phosphorylation of alphaB-crystallin in response to various types of stress. J. Biol. Chem. **272**, 29934-29941

12 Kato, K., Ito, H., Kamei, K., Inaguma, Y., Iwamoto, I. and Saga, S. (1998) Phosphorylation of alphaB-crystallin in mitotic cells and identification of enzymatic activities responsible for phosphorylation. J. Biol. Chem. **273**, 28346-28354

13 Hoover, H. E., Thuerauf, D. J., Martindale, J. J. and Glembotski, C. C. (2000) alpha B-crystallin gene induction and phosphorylation by MKK6-activated p38. A potential role for alpha B-crystallin as a target of the p38 branch of the cardiac stress response. J. Biol. Chem. **275**, 23825-23833

14 Chiesa, R., Gawinowicz-Kolks, M. A., Kleiman, N. J. and Spector, A. (1987) The phosphorylation sites of the B2 chain of bovine alpha-crystallin. Biochem. Biophys. Res. Commun. **144**, 1340-1347

15 Wang, K., Gawinowicz, M. A. and Spector, A. (2000) The effect of stress on the pattern of phosphorylation of alphaA and alphaB crystallin in the rat lens. Exp. Eye Res. **71**, 385-393

16 Ito, H., Iida, K., Kamei, K., Iwamoto, I., Inaguma, Y. and Kato, K. (1999) AlphaB-crystallin in the rat lens is phosphorylated at an early post-natal age. FEBS Lett. **446**, 269-272

17 Carver, J. A., Nicholls, K. A., Aquilina, J. A. and Truscott, R. J. (1996) Age-related changes in bovine alpha-crystallin and high-molecular-weight protein. Exp. Eye Res. **63**, 639-647

18 Miesbauer, L. R., Zhou, X., Yang, Z., Sun, Y., Smith, D. L. and Smith, J. B. (1994) Post-translational modifications of water-soluble human lens crystallins from young adults. J. Biol. Chem. **269**, 12494-12502

19 Mann, E., McDermott, M. J., Goldman, J., Chiesa, R. and Spector, A. (1991) Phosphorylation of alpha-crystallin B in Alexander's disease brain. FEBS Lett. **294**, 133-136

20 Pountney, D. L., Treweek, T. M., Chataway, T., Huang, Y., Chegini, F., Blumbergs, P. C., Raftery, M. J. and Gai, W. P. (2005) Alpha B-crystallin is a major component of glial cytoplasmic inclusions in multiple system atrophy. Neurotox. Res. **7**, 77-85

21 Wang, K. and Spector, A. (1996) Alpha-crystallin stabilizes actin filaments and prevents cytochalasin-induced depolymerization in a phosphorylation-dependent manner. Eur. J. Biochem. **242**, 56-66

22 Kamei, A., Hamaguchi, T., Matsuura, N. and Masuda, K. (2001) Does post-translational modification influence chaperone-like activity of alpha-crystallin? I. Study on phosphorylation. Biol. Pharm. Bull. **24**, 96-99

23 Ito, H., Kamei, K., Iwamoto, I., Inaguma, Y., Nohara, D. and Kato, K. (2001) Phosphorylation-induced change of the oligomerization state of alpha B-crystallin. J. Biol. Chem. **276**, 5346-5352

24 Aquilina, J. A., Benesch, J. L., Ding, L. L., Yaron, O., Horwitz, J. and Robinson, C. V. (2004) Phosphorylation of alphaB-crystallin alters chaperone function through loss of dimeric substructure. J. Biol. Chem. **279**, 28675-28680

25 Koteiche, H. A. and McHaourab, H. S. (2003) Mechanism of chaperone function in small heat-shock proteins. Phosphorylation-induced activation of two-mode binding in alphaB-crystallin. J. Biol. Chem. **278**, 10361-10367

26 Sunde, M. and Blake, C. (1997) The structure of amyloid fibrils by electron microscopy and X-ray diffraction. Adv. Protein Chem. **50**, 123-159

27 Jimenez, J. L., Nettleton, E. J., Bouchard, M., Robinson, C. V., Dobson, C. M. and Saibil, H. R. (2002) The protofilament structure of insulin amyloid fibrils. Proc. Natl. Acad. Sci. U. S. A. **99**, 9196-9201

28 Farrell, H. M., Jr., Cooke, P. H., Wickham, E. D., Piotrowski, E. G. and Hoagland, P. D. (2003) Environmental influences on bovine kappa-casein: reduction and conversion to fibrillar (amyloid) structures. J. Protein Chem. **22**, 259-273

29 Kammerer, R. A., Kostrewa, D., Zurdo, J., Detken, A., Garcia-Echeverria, C., Green, J. D., Muller, S. A., Meier, B. H., Winkler, F. K., Dobson, C. M. and Steinmetz, M. O. (2004) Exploring amyloid formation by a de novo design. Proc. Natl. Acad. Sci. U. S. A. **101**, 4435-4440

30 Horwitz, J., Huang, Q. L., Ding, L. and Bova, M. P. (1998) Lens alpha-crystallin: chaperone-like properties. Methods Enzymol. **290**, 365-383

31 Nielsen, L., Frokjaer, S., Brange, J., Uversky, V. N. and Fink, A. L. (2001) Probing the mechanism of insulin fibril formation with insulin mutants. Biochemistry **40**, 8397-8409

32 Sobott, F., Hernandez, H., McCammon, M. G., Tito, M. A. and Robinson, C. V. (2002) A tandem mass spectrometer for improved transmission and analysis of large macromolecular assemblies. Anal. Chem. **74**, 1402-1407

33 Aquilina, J. A., Benesch, J. L., Bateman, O. A., Slingsby, C. and Robinson, C. V. (2003) Polydispersity of a mammalian chaperone: mass spectrometry reveals the population of oligomers in alphaB-crystallin. Proc. Natl. Acad. Sci. U. S. A. **100**, 10611-10616

34 Treweek, T. M., Rekas, A., Lindner, R. A., Walker, M. J., Aquilina, J. A., Robinson, C. V., Horwitz, J., Perng, M. D., Quinlan, R. A. and Carver, J. A. (2005) R120G alphaB-crystallin promotes the unfolding of reduced alpha-lactalbumin and is inherently unstable. FEBS J. **272**, 711-724

35 Carver, J. A. and Lindner, R. A. (1998) NMR spectroscopy of alpha-crystallin. Insights into the structure, interactions and chaperone action of small heat-shock proteins. Int. J. Biol. Macromol. **22**, 197-209

36 Thorn, D. C., Meehan, S., Sunde, M., Rekas, A., Gras, S. L., Macphee, C. E., Dobson, C. M., Wilson, M. R. and Carver, J. A. (2005) Amyloid fibril formation by bovine milk kappa-casein and its inhibition by the molecular chaperones alpha(S)- and beta-casein. Biochemistry **44**, 17027-17036

37 Farahbakhsh, Z. T., Huang, Q. L., Ding, L. L., Altenbach, C., Steinhoff, H. J., Horwitz, J. and Hubbell, W. L. (1995) Interaction of alpha-crystallin with spin-labeled peptides. Biochemistry **34**, 509-516

38 Horwitz, J. (2005) in Protein folding handbook. Part II. (Buchner, J. and Kiefhaber, T., eds.), pp. 858-875, Wiley-VCH, Weinheim

39 den Engelsman, J., Bennink, E. J., Doerwald, L., Onnekink, C., Wunderink, L., Andley, U. P., Kato, K., de Jong, W. W. and Boelens, W. C. (2004) Mimicking phosphorylation of the small heat-shock protein alphaB-crystallin recruits the F-box protein FBX4 to nuclear SC35 speckles. Eur. J. Biochem. **271**, 4195-4203

40 den Engelsman, J., Gerrits, D., de Jong, W. W., Robbins, J., Kato, K. and Boelens, W. C. (2005) Nuclear import of alpha B-crystallin is phosphorylation-dependent and hampered by hyperphosphorylation of the myopathy-related mutant R120G. J. Biol. Chem. **280**, 37139-37148

41 Cacace, M. G., Landau, E. M. and Ramsden, J. J. (1997) The Hofmeister series: salt and solvent effects on interfacial phenomena. Q. Rev. Biophys. **30**, 241-277

42 van Montfort, R. L., Basha, E., Friedrich, K. L., Slingsby, C. and Vierling, E. (2001) Crystal structure and assembly of a eukaryotic small heat shock protein. Nat. Struct. Biol. **8**, 1025-1030

43 LeVine, H., 3rd. (1999) Quantification of beta-sheet amyloid fibril structures with thioflavin T. Methods Enzymol. **309**, 274-284

44 Rekas, A., Adda, C. G., Andrew Aquilina, J., Barnham, K. J., Sunde, M., Galatis, D., Williamson, N. A., Masters, C. L., Anders, R. F., Robinson, C. V., Cappai, R. and Carver, J. A. (2004) Interaction of the molecular chaperone alphaB-crystallin with alpha-synuclein: effects on amyloid fibril formation and chaperone activity. J. Mol. Biol. **340**, 1167-1183

45 Hatters, D. M., Lindner, R. A., Carver, J. A. and Howlett, G. J. (2001) The molecular chaperone, alpha-crystallin, inhibits amyloid formation by apolipoprotein C-II. J. Biol. Chem. **276**, 33755-33761

46 Sathish, H. A., Stein, R. A., Yang, G. and McHaourab, H. S. (2003) Mechanism of chaperone function in small heat-shock proteins. Fluorescence studies of the conformations of T4 lysozyme bound to alphaB-crystallin. J. Biol. Chem. **278**, 44214-44221

47 Bova, M. P., Yaron, O., Huang, Q., Ding, L., Haley, D. A., Stewart, P. L. and Horwitz, J. (1999) Mutation R120G in alphaB-crystallin, which is linked to a desmin-related myopathy, results in an irregular structure and defective chaperone-like function. Proc. Natl. Acad. Sci. U. S. A. **96**, 6137-6142

48 Koteiche, H. A. and McHaourab, H. S. (2006) Mechanism of a hereditary cataract phenotype: Mutations in alpha A-crystallin activate substrate binding. J. Biol. Chem. **281**, 14373-14379

Biochemical Journal Immediate Publication. Published on 23 Aug 2006 as manuscript BJ20060981

Figure Legends

Fig. 1 Mimicking phosphorylation of αB-crystallin affects its structure as monitored by fluorescence spectroscopy.

Intrinsic tryptophan fluorescence at 37°C (A) and 60°C (B), ANS fluorescence at 37°C (C) and 60°C (D) and FRET analysis at 37°C (E) and 60°C (F) of αB-WT (filled diamonds), αB-1P (filled triangles), αB-2P (open diamonds) and αB-3P (open squares). The proteins (100 μg/mL) were incubated in 50 mM phosphate buffer, pH 7.2 at each temperature for 30 mins before the spectra were measured.

Fig. 2 The oligomeric distribution of αB-WT and αB-3P.

(A) Nanospray mass spectra of αB-WT and αB-3P. The peaks at 10,080 and 10,200 *m/z*, corresponding to species with two charges per subunit for αB-WT and αB-3P respectively, were isolated and subjected to collision-induced dissociation. The doubly stripped oligomers were used to calculate the oligomeric distribution of the intact proteins as described previously [24]. (B) Histograms quantifying the relative abundance of the various oligomeric species for αB-WT and αB-3P.

Fig. 3 Phosphorylation mimics of αB-crystallin are more effective at preventing amyloid fibril formation by RCMκ-casein.

(A) Thioflavin T (ThT) binding curves of RCMκ-casein (500 μg/mL) incubated at 37°C in 50 mM phosphate buffer, pH 7.2 in the absence (filled squares) or presence of αB-WT (filled diamonds), αB-1P (filled triangles), αB-2P (open diamonds), or αB-3P (open squares). The chaperone was at 500 μg/mL and the ThT fluorescence was monitored by an *in situ* assay for 15 h. The change in ThT fluorescence of each sample is shown. This experiment was performed four times and the data shown are representative. (B) SEC of RCMκ-casein before and after fibril formation and after incubation in the presence of αB-WT and αB-3P. The proteins were loaded on to a Superdex 200HR 10/30 column and eluted in 50 mM phosphate buffer, pH 7.2 at a flow rate of 0.4mL/min. Calibration of the column was performed using (1) blue dextran; void, Vd, (2) thyroglobulin; 670 kDa, (3) γ-globulin; 158 kDa, (4) ovalbumin; 44 kDa and (5) myoglobulin; 17 kDa.

Fig. 4 Fibril formation by RCMκ-casein in the presence of αB-crystallin.
Electron micrographs of RCMκ-casein (500 μg/mL) after incubation at 37°C in 50 mM phosphate buffer, pH 7.2 for 15 h in the absence (A) or presence of αB-WT (B) or αB-3P (C). The chaperone was present at 500 μg/mL. Scale bar represents 500 nm.

Fig. 5 Mimicking phosphorylation of αB-crystallin decreases its ability to prevent amyloid fibril formation by ccβ-Trp.
(A) Thioflavin T (ThT) binding curves of ccβ-Trp (150 μg/mL) incubated at 37°C in 50 mM phosphate buffer, pH 7.8 in the absence (filled squares) or presence of αB-WT (filled diamonds), αB-1P (filled triangles), αB-2P (open diamonds), or αB-3P (open squares). The chaperone was at 130 μg/mL and the ThT fluorescence was monitored by an *in situ* assay for 15 h. The change in ThT fluorescence of each sample is shown. (B) After the ThT assay, the insoluble (pellet) fractions were separated and the proteins resolved by SDS-PAGE. This experiment was performed a minimum of three times and the data shown are representative.

Fig. 6 Fibril formation by ccβ-Trp in the presence of αB-crystallin.
Electron micrographs of ccβ-Trp (150 μg/mL) after incubation at 37°C in 50 mM phosphate buffer, pH 7.8 for 15 h in the absence (A) or presence of αB-WT (B and C) or αB-3P (D and E). The chaperone was present at 130 μg/mL. Scale bar represents 500 nm.

Fig. 7 Phosphorylation mimics of αB-crystallin are more effective at preventing the heat-induced amorphous aggregation of target proteins.
Aggregation curves of (A) β_L-crystallin (500 μg/mL) and (C) catalase incubated at 60°C in 50 mM phosphate buffer, pH 7.2 and of (E) alcohol dehydrogenase incubated at 42°C in 50 mM phosphate buffer, pH 7.2 containing 100 mM NaCl and 2 mM EDTA. The target proteins were incubated in the absence (filled squares) or presence of αB-WT (filled diamonds), αB-1P (filled triangles), αB-2P (open diamonds), or αB-3P (open squares) and the change in light scattering measured at 340 nm. In A and C, the chaperones were added at a final concentration of 100 μg/mL; in E they were

added at a final concentration of 50 μg/mL. (B, D and F) After the aggregation assay, the soluble and insoluble fractions were separated and the proteins resolved by SDS-PAGE. Each experiment was performed a minimum of three times and data shown are representative.

Fig. 8 The effect of mimicking phosphorylation of αB-crystallin on its chaperone ability to prevent DTT-induced amorphous aggregation of target proteins.

Aggregation curves of (A) insulin (250 μg/mL) and (C and E) α-lactalbumin (500 μg/mL) incubated in the absence (filled squares) or presence of αB-WT (filled diamonds), αB-1P (filled triangles), αB-2P (open diamonds), or αB-3P (open squares). (A) Insulin was incubated at 37°C in 50 mM phosphate buffer, pH 7.2 with 10 mM DTT. α-Lactalbumin was incubated at 37°C in (C) 50 mM phosphate buffer, pH 7.2 containing 100 mM NaCl with 20 mM DTT, or (E) 100 mM ammonium acetate buffer, pH 6.8 with 20 mM DTT. In each case, the chaperone (250 μg/mL) was added to the reaction mixture and the change in light scattering measured at 340 nm. (B, D and F) After the aggregation assay, the soluble and insoluble fractions were separated and the proteins resolved by SDS-PAGE. Each experiment was performed a minimum of three times and the data shown are representative.

Fig. 9 The effect of solution condition on the thermal stability and oligomeric distribution of αB-WT and αB-3P.

Thermal denaturation curves of αB-WT (filled diamonds) and αB-3P (open squares) in 50 mM phosphate buffer, pH 7.2 containing 100 mM NaCl (A) and 100 mM ammonium acetate buffer, pH 6.8 (B). The proteins were incubated at 250 μg/mL and the temperature increased at the rate of 1°C min^{-1}. Precipitation of the proteins was monitored by measuring the change in light scattering at 360 nm. (C) SEC coupled to multiangle laser light scattering. αB-WT and αB-3P (1.5 mg/mL) were loaded on to a Superose 6HR 10/30 column and eluted with 100 mM ammonium acetate, pH 6.8 at a flow rate of 0.5 mL/min. The solid lines represent the absorption profile of the eluted protein and circles represent the molecular mass obtained as a function of the elution volume.

Biochemical Journal Immediate Publication. Published on 23 Aug 2006 as manuscript BJ20060981

Fig. 1

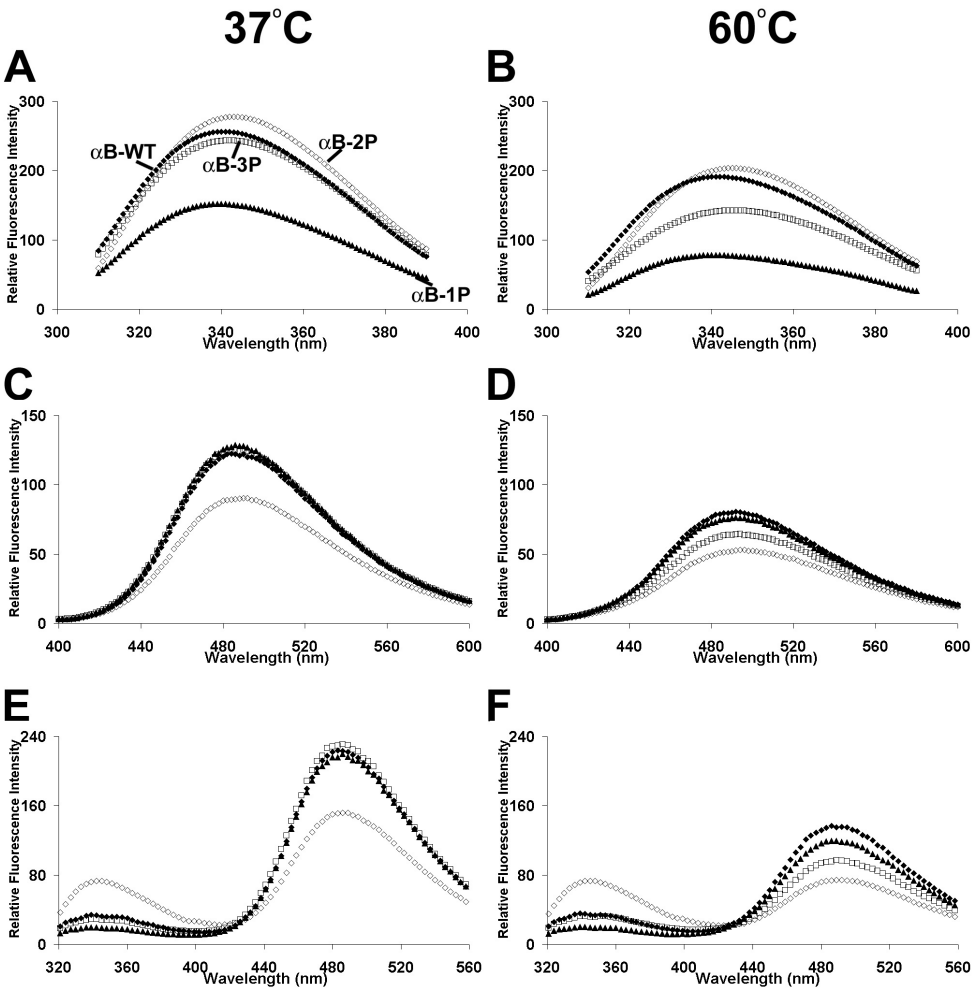

Biochemical Journal Immediate Publication. Published on 23 Aug 2006 as manuscript BJ20060981

Fig. 2

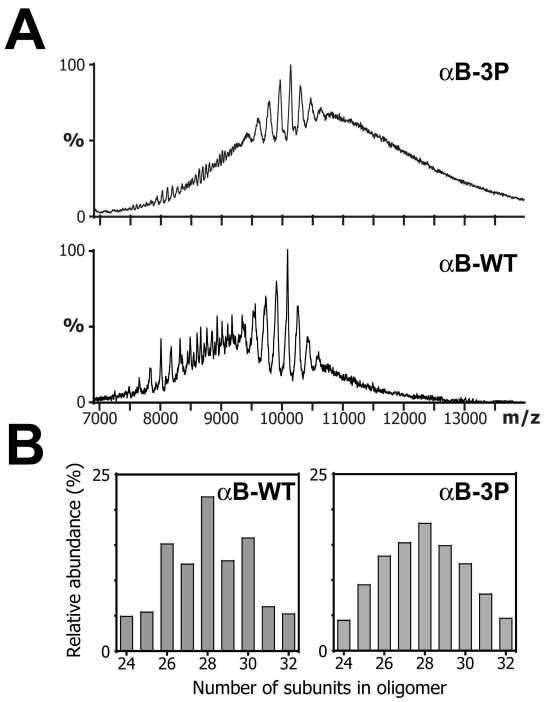

Fig. 3

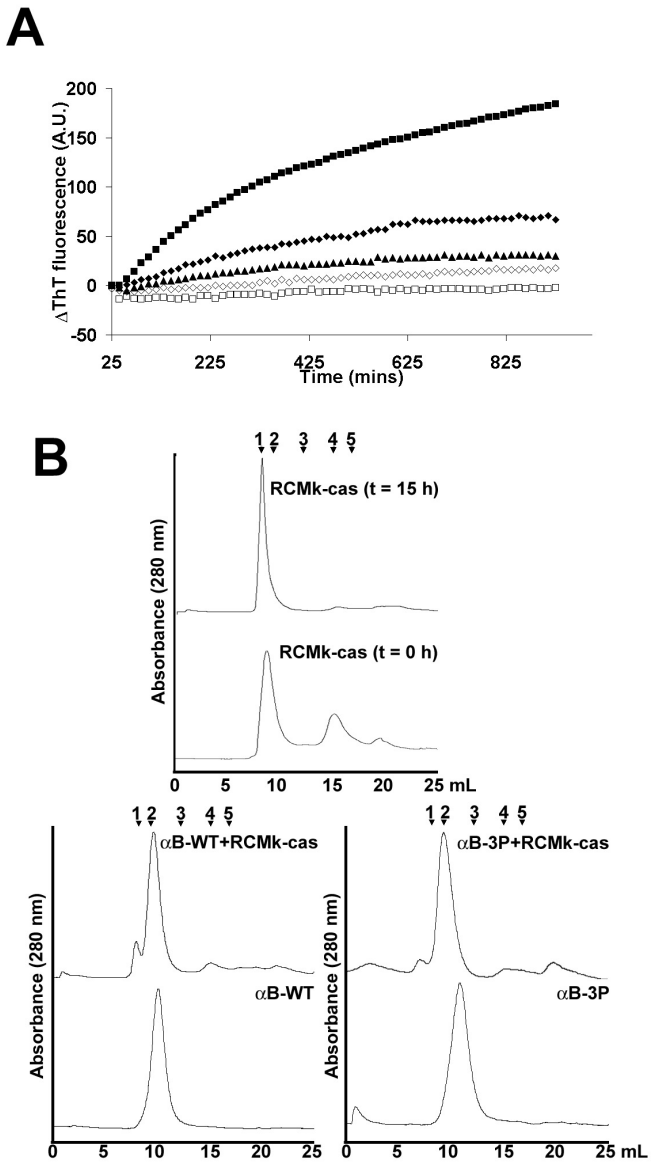

Biochemical Journal Immediate Publication. Published on 23 Aug 2006 as manuscript BJ20060981

Fig. 4

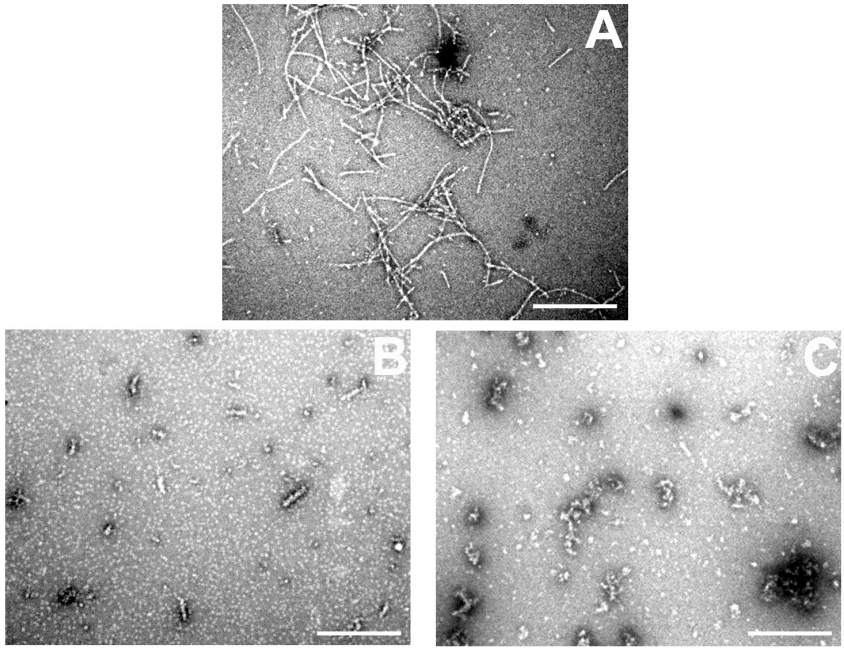

Biochemical Journal Immediate Publication. Published on 23 Aug 2006 as manuscript BJ20060981

Fig. 5

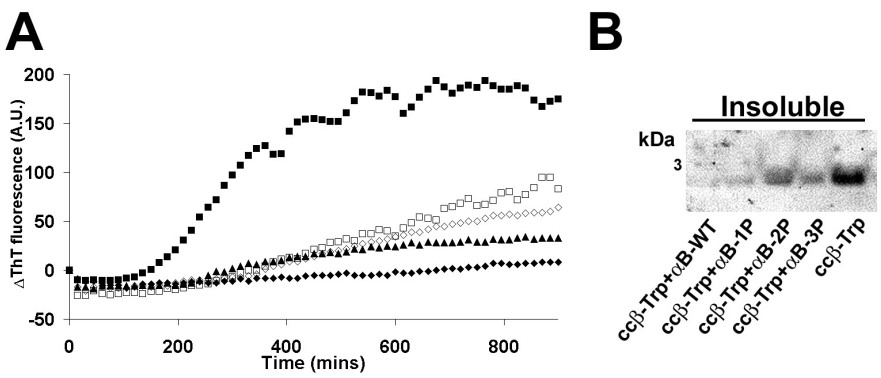

Biochemical Journal Immediate Publication. Published on 23 Aug 2006 as manuscript BJ20060981

Fig. 6

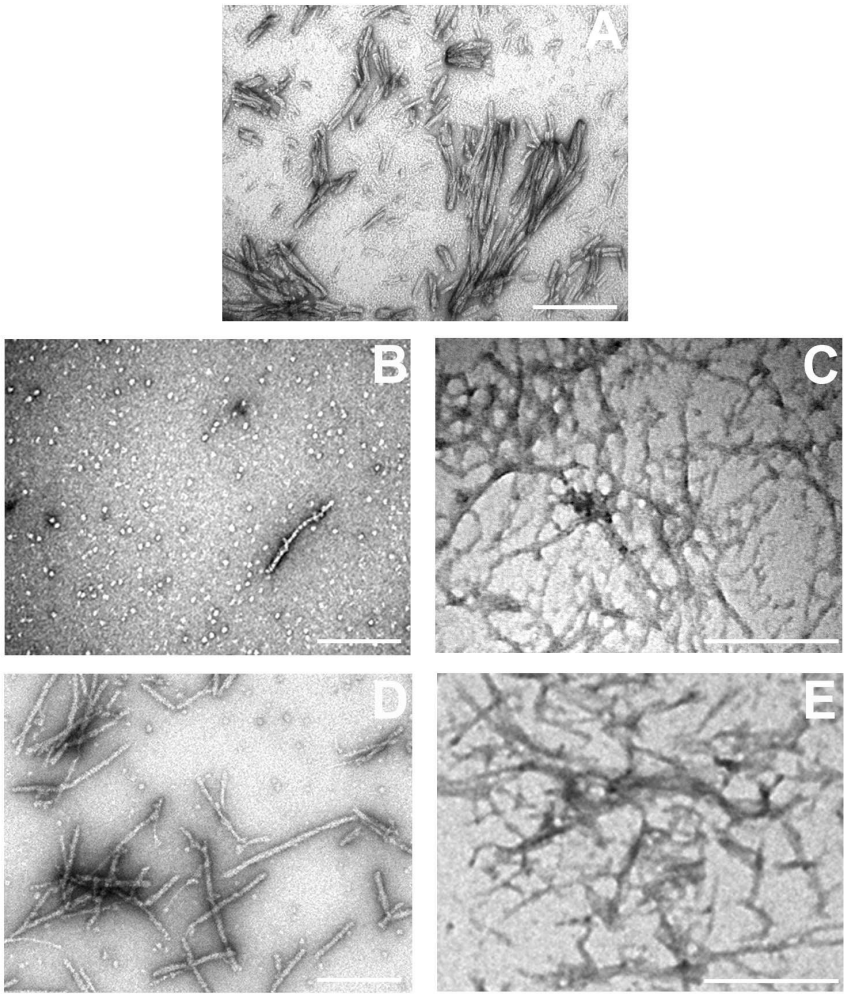

Biochemical Journal Immediate Publication. Published on 23 Aug 2006 as manuscript BJ20060981

Fig. 7

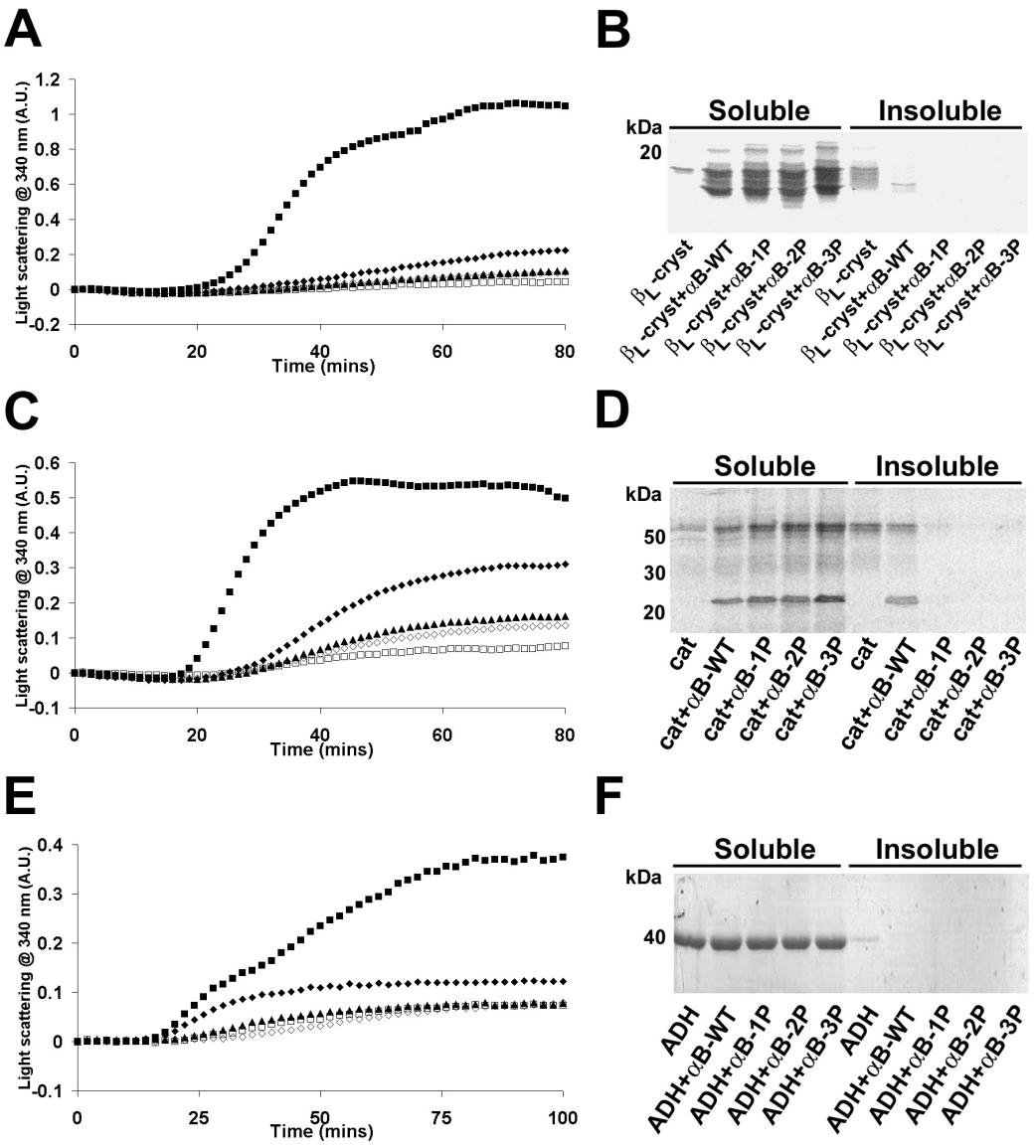

Biochemical Journal Immediate Publication. Published on 23 Aug 2006 as manuscript BJ20060981

Fig. 8

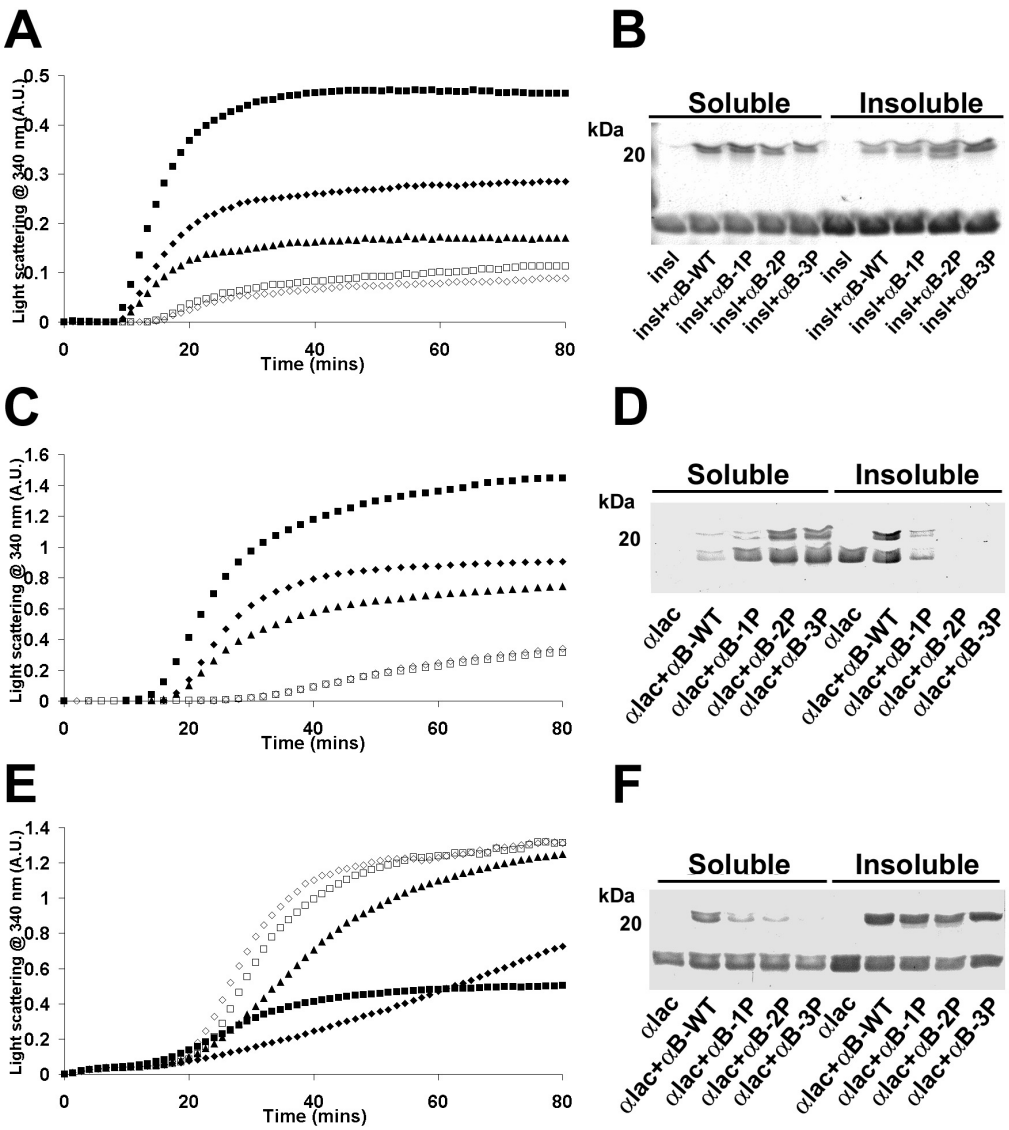

Biochemical Journal Immediate Publication. Published on 23 Aug 2006 as manuscript BJ20060981

Fig. 9